Quantum molecular dynamics simulations of shocked nitrogen oxide

S. Mazevet,[1] P. Blottiau,[2] J. D. Kress,[1] and L. A. Collins[1]
[1]*Theoretical Division, Los Alamos National Laboratory, Los Alamos, New Mexico 87545, USA*
[2]*CEA/DIF, Boîte Postale 12 Bruyère Le Chatel, France*
(Received 7 January 2004; published 22 June 2004)

Using quantum molecular dynamics, we study the dissociation of nitrogen oxide along the principal and reshocked Hugoniots. We obtain good agreement with available experimental data for the first and highest second-shock Hugoniots. Reminiscent of the experimental and theoretical findings for shocked liquid nitrogen, the calculation indicates little temperature variation along the second shock as the fluid dissociates. The analysis of the concentration of molecular species along both Hugoniots indicates, as expected, that for low final shock densities molecular nitrogen is forming when nitrogen oxide dissociates. In contrast to basic assumptions used for high pressure modeling of nitrogen oxide, we find, however, that oxygen mostly stays in an atomic state for the whole density-temperature range studied.

DOI: 10.1103/PhysRevB.69.224207 PACS number(s): 71.15.Pd, 62.50.+p, 61.20.Ja

I. INTRODUCTION

The study of materials under extreme conditions of temperature and pressure has made significant progress in the past few years, due to noticeable advances in both the experimental and theoretical techniques. On the experimental side, *Z* pinch and laser-driven experimental setups have pushed Hugoniot measurements into the megabar range.[1,2] On the theoretical side, simulation methods, such as quantum molecular dynamics and path-integral Monte Carlo,[3–7] now allow the study of materials under such conditions from a mostly *ab initio* standpoint. However, the application of these methods has up to now primarily focused on pure systems such as hydrogen, nitrogen, and oxygen, and lately on complementing the study of the equation of state (EOS) with the determination of the associated optical and electrical properties.[8–12]

In the present work, we study the EOS and dissociation of NO along the principal and second-shock Hugoniots using quantum molecular dynamics (QMD). While NO presents a natural extension to study the EOS of multicomponent systems,[13] it also serves as a prototype for the study of explosive compounds and their associated reactive chemistry. Furthermore, the determination of reactive potentials,[14,15] necessary for the study of technologically relevant and more complex systems such as H-C-N-O, also requires first a calibration to the NO system. Up to now, this calibration has been solely supported by the experimental measurements of the first (principal) and second-shock Hugoniots.[13] To complement the latter, we first calculate the principal and second-shock Hugoniots as well as the corresponding temperature up to pressures of, respectively, 83 GPa and 65 GPa.

We further paid particular attention to the constituency of the fluid along each Hugoniot as the chemistry induced by such an increase of pressure and temperature remains among the most challenging aspects in the modeling of such systems. Quantum molecular dynamics methods, where the electrons receive a fully quantum mechanical treatment, are particularly suited for the study of such chemical processes as ionization, recombination, dissociation, and association of the various atomic species present in the media, as well as many-body effects, which are treated on an equal footing within the framework of the density-functional theory (DFT). Using this parameter-free method, we show that for these overdriven experiments, where the shock front propagates faster than the reaction front, the dissociation of nitrogen oxide leads, as expected, to the formation of molecular nitrogen at the lowest density. In contrast, we find that oxygen mostly stays in an atomic state for the density-temperature range covered by the principal and highest second-shock Hugoniots. This challenges the basic assumption used in the modeling of the high-pressure behavior of nitrogen oxide[13,16] where molecular nitrogen and molecular oxygen are both assumed to be the only products of the reaction.

II. PRINCIPAL AND RESHOCKED HUGONIOTS

In the present application, the molecular dynamics trajectories were calculated using the VASP plane-wave pseudopotential code, which was developed at the Technical University of Vienna.[17] This code implements the Vanderbilt ultrasoft pseudopotential scheme[18] in a form supplied by Kresse and Hafner[19] and the Perdew-Wang 91 parametrization of the generalized gradient approximation (GGA).[20] Trajectories were calculated at fixed volume and at separate density and temperature points, selected to span a range of densities from $\rho=1.90$ to $\rho=3.2$ g/cm^3 and temperatures from $T=1000$ K to $T=14\,000$ K to highlight the first and second-shock Hugoniot regions. We used both 27/27 and 54/54 nitrogen/oxygen atoms in the unit cell and fixed the plane-wave cutoff at 495 eV. All the simulations were started using molecular NO as initial conditions. Integration of the equations of motion proceeded with time steps of 2 fs and for a total simulation time of up to 6 ps. During the simulations, the ion temperature T_i was kept constant at every time step using velocity scaling. The validity of this assumption for the calculation of Hugoniot points was tested for the case of nitrogen using microcanonical simulations.[22] In turn, the assumption of local thermodynamical equilibrium sets the

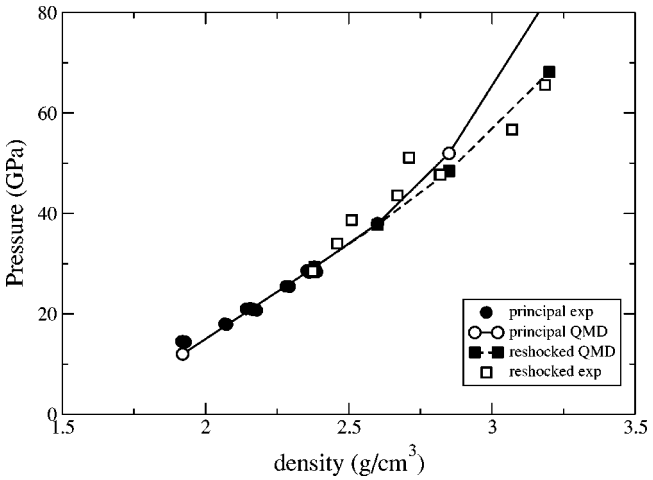

FIG. 1. Principal and reshocked NO Hugoniots. The scatter of the experimental points at a given density are representative of the experimental error bars.

electron temperature T_e to that of the ions T_i, and electronic eigenstates occupied according to a Fermi-Dirac distribution. We employed up to 225 and 350 electronic states for simulations using, respectively, 54 and 108 atoms. Additional tests indicated that this choice gave very good convergence in energies and properties. Additional details on the trajectory calculations can be found in Refs. 21 and 22.

The Rankine-Hugoniot equation[23]

$$(U_0 - U_1) + \tfrac{1}{2}(V_0 - V_1)(P_0 + P_1) = 0 \qquad (1)$$

describes the shock adiabat through a relation between the initial and final volume, internal energy, and pressure, respectively, (V_0, U_0, P_0) and (V_1, U_1, P_1). As described in Ref. 21, to calculate the Hugoniot point for a given V_1 and a set of T_1's, the DFT-MD P and U for a fixed V_1 were least-squares fit to a quadratic function in T. P_1 and T_1 were determined by substituting these functions and solving Eq. (1). For the principal Hugoniot, we have chosen, in accordance with the experimental measurements, the initial conditions $P_0=0$ and $\rho_0=1.22$ g/cm^3. The reference energy, $U_0=-5.87$ eV/atom, was selected such that the energy of the isolated NO molecule, with an internuclear distance of $2.175a_B$, is zero ($1a_B=1$ a.u.). For the reshocked Hugoniot, we concentrated on the initial conditions corresponding to the highest first-shock Hugoniot point obtained experimentally, $\rho=2.38$ g/cm^3. In this case we choose as initial conditions for the Rankine-Hugoniot equation (1), $P_0=29.3$ GPa and $U_0=-5.017$ eV/atom as given by the QMD calculations for a density of $\rho=2.38$ g/cm^3.

In Fig. 1, we compare directly the results of the QMD calculations with the available experimental measurements[13] for the first and highest second shocks. For the first shock, we choose to plot the individual measurements instead of the averaged ones as the highest density points represent the initial conditions for the second shock points that will be discussed below. For the highest density reached experimentally along the first shock, $\rho=2.38$ g/cm^3, we find a remarkable agreement between the calculations and the measurements. The QMD pressure at this density is $P=29.3$ GPa using 108 atoms in the simulation cell and compares well with the experimental one, $P=28.47$ GPa. This agreement carries over to the particle and shock velocities where we obtain $u_p=3.29$ km s^{-1} and $u_s=7.02$ km s^{-1} compared to the experimental results of, respectively, 3.245 and 6.94 km s^{-1}. The agreement along the first-shock Hugoniot holds as the density is lowered, with a QMD pressure of 12.1 GPa at the lowest density measured which compares rather well with the experimental pressure of 14.47 GPa.

We find a rather small dependence on the number of particles used in the simulation cell for the pressures calculated at these two Hugoniot points. For the lowest density point, 1.92 g/cm^3, we obtain a pressure of 11.5 GPa using 54 atoms in the unit cell which compares well with the value of 12.1 GPa given above and obtained using 108 atoms. At a density of 2.38 g/cm^3, the Hugoniot pressures obtained using 54 and 108 atoms in the simulation cell are, respectively, 29.7 and 29.3 GPa. Simulations using 54 atoms at a density of 1.92 g/cm^3 also show little sensitivity to the inclusion of spin in the calculation of the internal energy and final pressure. This suggests that the simulations performed without accounting for spin and using 108 atoms in the simulation cell for the lowest density provide well-converged Hugoniot points.

We find that the largest source of uncertainty in the calculation of the Hugoniot points comes from the choice of the zero of energy in relation (1). Ideally, the zero of energy should be obtained by performing a simulation at the experimental initial conditions of 1.263 g/cm^3 and $T=122$ K and corrected for the classical description of the nuclei. Both the density, which leads to a large number of plane waves, and the temperature, which requires long simulation time to equilibrate, make such a simulation out of reach with current computational capabilities. This results in some ambiguities in the choice of the zero of energy. For the present calculations, we take, as reference, the energy of the isolated NO molecule at the experimental internuclear distance of $2.175a_B$ calculated with the Vanderbilt ultrasoft potential. While accounting for spin affects the zero of energy by -0.2 eV/atom, we made the choice of calculating the zero of energy using the same ultrasoft potential and using the same assumptions (i.e., without spin) as the ones used in the subsequent simulations. This choice is motivated by the fact that the Hugoniot relation (1) indicates that Hugoniot points are determined by the internal energy change between the two end points rather than the absolute internal energy of either the initial or final state. This choice only affects the Hugoniot point at the lowest density. At 2.38 g/cm^3, the agreement between the calculated and measured Hugoniot points is only marginally affected by the particular choice for the zero of energy.

For the second-shock Hugoniot, we plotted as experimental results the pressure points obtained for the highest first-shock densities, between 2.28 and 2.38 g/cm^3. The theoretical second-shock Hugoniot is calculated using the QMD results obtained for the principal Hugoniot at a density of $\rho=2.38$ g/cm^3 only. Such a small variation in the initial conditions does not affect substantially the final second-shock pressures. This variation does not, for example, explain the

TABLE I. Hugoniot points derived from GGA-MD simulation for a final density ρ. First (P_1, T_1) and second (P_2, T_2) Hugoniots for initial conditions as discussed in the text.

ρ_1(g/cm^3)	P_1(GPa)	T_1(K)	P_2(GPa)	T_2(K)
1.92	12.1	3194		
2.38	29.3	4979		
2.6	37.9	6000	37.7	5217
2.85	52.0	6890	48.4	5278
3.2	83.4	10452	68.2	5794

consistently higher experimental pressures measured for the second shock at densities between 2.5 and 2.75 g/cm^3. A closer inspection of Fig. 1 also reveals a significant scatter in the experimental data for this density range and an improved agreement as the density increases. These two points combined with the good description of the first-shock Hugoniot, suggest that QMD provides a satisfactory description of the state of the fluid as the simultaneous increase in pressure and temperature breaks the molecular bonds.

In Table I, we report the calculated temperature for the first and second-shock Hugoniots. We see that along the principal Hugoniot the increase in temperature presents a plateau for densities between 2.6 and 2.85 g/cm^3. This behavior is usually indicative of the dissociation of molecular species in the media and suggests that NO is dissociating in this density region. For the second-shock Hugoniot studied here, the calculations indicate that the temperature is only increasing by about 10% while the corresponding pressure varies by almost two and a half times. Such a behavior in the second shock was found both theoretically and experimentally for shocked liquid nitrogen.[22,24,25] Nitrogen is the diatomic system with the highest isolated dissociation energy and as such presents a significant energy sink in the density region where it dissociates. As the nitrogen oxide dissociation energy is comparable to that of nitrogen, it is reasonable to assume that a similar argument holds in the present case and that the increase in energy during the second shock is absorbed in breaking the molecular bonds rather than transferred as kinetic energy. This also suggests that the end products of the reaction, molecular nitrogen and oxygen, also dissociate and present a significant energy sink in this density region.

III. CONSTITUENCY ANALYSIS

To quantify the state of the fluid as the density increases, we calculate the pair-correlation functions of each possible diatomic species, NO, O_2, and N_2. Figure 2 shows such a result along the first Hugoniot and extending beyond the density range explored experimentally. At the lowest density $\rho = 1.92$ g/cm^3, the nitrogen oxide and nitrogen correlation functions, $g_{\text{N-O}}(r)$ and $g_{\text{N-N}}(r)$, peak at around $2a_B$, corresponding to the equilibrium internuclear distances of the NO and N molecules, respectively, $r_{\text{N-O}} = 2.17a_B$ and $r_{\text{N-N}} = 2.06a_B$. The pair-correlation functions at 1.92 g/cm^3 indicate that the NO fluid has partially dissociated and is constituted of a mixture of NO and N_2 molecules. At this density,

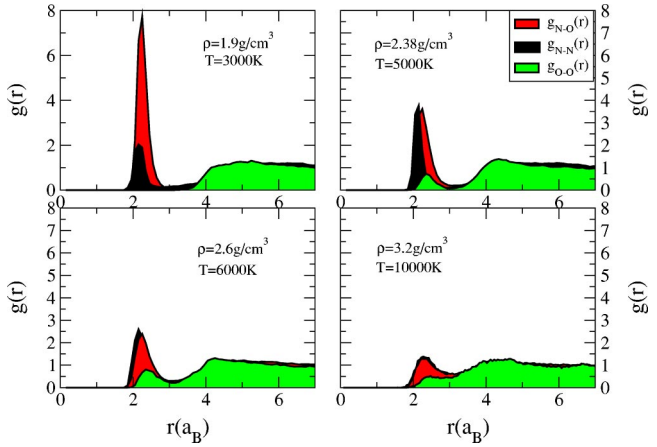

FIG. 2. (Color online) Pair-correlation functions along the principal NO Hugoniot.

the oxygen correlation function $g_{\text{O-O}}(r)$ does not show a maximum at a distance corresponding to the equilibrium distance of the oxygen molecule $r_{\text{O-O}} = 2.282a_B$. This indicates that, in contrast to nitrogen, oxygen does not recombine significantly upon the dissociation of NO at this density. As the density increases to $\rho = 2.38$ g/cm^3, the sizable reduction and broadening of the maxima of $g_{\text{N-O}}(r)$ around $2a_B$ shows that as both the density and temperature increase, NO molecules now significantly dissociate. In contrast, the $g_{\text{N-N}}(r)$ pair-correlation function at this density indicates that upon dissociation of NO, nitrogen recombines significantly to form molecules. While a maximum at around $2a_B$ is now also noticeable for the $g_{\text{O-O}}(r)$ pair correlation function at this density, its small magnitude suggests that in contrast to nitrogen, oxygen mostly stays in an atomic state at this density. As the density is further increased to 2.6 g/cm^3, the reduction and broadening of the maxima of the three pair-correlation functions indicate that all of the molecular systems further dissociate. Figure 2 shows that this trend continues up to a density of 3.2 g/cm^3. At the highest density considered here, both NO and N_2 have almost completely dissociated. Molecular nitrogen still represents a significant fraction of the total number of molecular systems left in the sample while oxygen mostly stays in an atomic state.

This finding challenges the conventional assumption used to model the dissociation of nitrogen oxide along both the principal and reshocked Hugoniot.[13,16] When modeling the high-pressure behavior of nitrogen oxide, it is generally assumed that the dissociation of NO leads to nitrogen and oxygen in a molecular state. This assumption is likely to be valid when the media is shocked to low final densities, but the simulations performed here suggest that this is no longer the case for overdriven shocks. For such shocks, the shock front propagates faster than the reaction front, and the simulations performed here suggest that density effects on the end products of the reaction need to be taken into account in the modeling of the reaction.

As the pair-correlation functions shown in Fig. 2 can be sensitive to various assumptions used to perform the simulations, we show in Fig. 3 a sensitivity analysis on the number of particles used and on the inclusion of spin in the calcula-

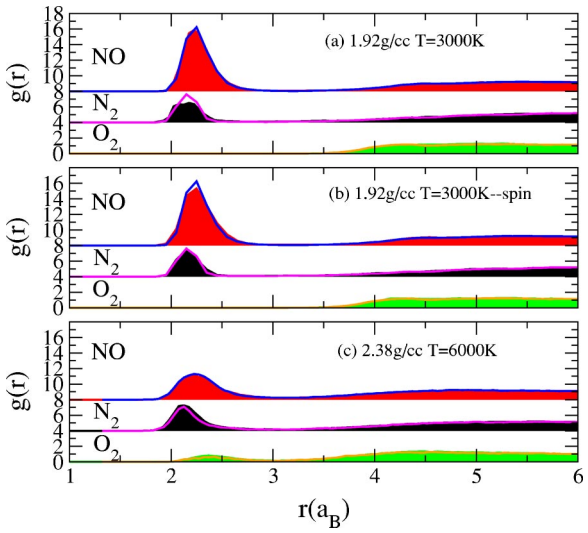

FIG. 3. (Color online) (a), (c) Sample size dependence of the constituency analysis. $g_{N\text{-}O}(r)$ 108 atoms (filled red), $g_{N\text{-}N}(r)$ 108 atoms (filled black), $g_{O\text{-}O}(r)$ 108 atoms (filled green), $g_{N\text{-}O}(r)$ 54 atoms (blue), $g_{N\text{-}N}(r)$ 54 atoms (pink), $g_{O\text{-}O}(r)$ 54 atoms (orange). (b) Spin dependence: $g_{N\text{-}O}(r)$ 54 atom nonspin (filled red), $g_{N\text{-}N}(r)$ 54 atom nonspin (black), $g_{O\text{-}O}(r)$ 54 atom nonspin (filled green), $g_{N\text{-}O}(r)$ 54 atom spin (blue), $g_{N\text{-}N}(r)$ 54 atom spin (pink), $g_{O\text{-}O}(r)$ 54 atom spin (orange). $g_{N\text{-}O}(r)$ and $g_{N\text{-}N}(r)$ are shifted by 8 and 4 for clarity.

tions. In Figs. 3(a) and 3(c), we show the sensitivity of the pair-correlation functions using a total of 54 and 108 atoms, at the two lowest densities along the principal Hugoniot. For the lowest density, Fig. 3(a), we show that the pair-correlation functions are not significantly sensitive to the number of particles used in the simulation. This sensitivity is the most noticeable for the nitrogen correlation functions and indicates that the increase in the number of particles in the simulation cell may affect the precise evaluation of the number of nitrogen molecules forming at a given density-temperature point. More importantly, this increase in particle number does not affect significantly the oxygen pair-correlation function which is still representative of oxygen in a mostly atomic state. In Fig. 3(b), we show at this same density and temperature that the constituency analysis is not sensitive to the inclusion of spin in the simulation. When using a total of 54 atoms, the various pair-correlation functions are rather similar when the total trajectory is calculated with and without spin. Finally, in Fig. 3(c), we show that the cell size dependence mostly disappear as the density and temperature increase along the Hugoniot and is only noticeable for the lowest density considered here.

As a final check of our simulations, we also compared the properties of the isolated molecules, as calculated within the DFT framework, with experimental data.[28] We performed the GGA calculations of the molecular properties using both the Gaussian chemistry package[27] (with a 6-31+G* basis) and the VASP QMD package used in the present work. The former implements a Gaussian basis set representation while the latter uses plane waves. Table II shows that in both cases, the molecular properties obtained (frequencies ω_e and bond distances r_e) are in excellent agreement with the experimental data. While the GGA dissociation energies are only within 2–15% of the experimental values, the trend in bond strength is clearly maintained with $D_e(O_2) < D_e(NO) < D_e(N_2)$. This suggests that the basic properties of the various molecular species are properly described within the bounds of the GGA method used in the present study.

The sensitivity analysis shows that the number of atoms used in the simulations provides a satisfactory description of the pair-correlation functions, especially for the highest densities studied here. While the exact concentration of each species and the formation of larger molecular systems could only be checked with simulations using an even larger number of particles, the results presented here clearly suggest, however, that molecular oxygen is hardly present at the density-temperature conditions corresponding to the principal Hugoniot. The variation of the molecular fraction of each species along the principal Hugoniot can be partially understood by an inspection of the various dissociation energies. Nitrogen has the highest dissociation energy of the molecular species considered here and, as such, is expected to be the molecular system most likely to be present in the sample as both the density and temperature increase. Furthermore, that oxygen has a lower dissociation energy than nitrogen oxide also suggests that oxygen is less likely to associate for density-temperature conditions where NO is dissociated. While this argument, based on the dissociation energy of the isolated molecular species, explains the overall trend of the

TABLE II. Comparison of the GGA isolated molecule properties with experimental data (Ref. 28).

		r_e(Ang)	ω_e(cm^{-1})(eV)	D_e(eV)	D_e (error)
N_2	PW91-Gaussian	1.1151	2362	10.24	(+1.9%)
	Expt.	1.0977	2359	10.05	
	PW91-VASP	1.111	2399	9.91	(−1.4%)
O_2	PW91-Gaussian	1.2281	1560	6.11	(+15%)
	Expt.	1.2075	1580	5.31	
	PW91-VASP	1.237		5.89	(+9%)
NO	PW91-Gaussian	1.1684	1897	7.28	(+8.2%)
	Expt.	1.1508	1904	6.73	
	PW91-VASP	1.171	1873	6.88	(+2.2%)

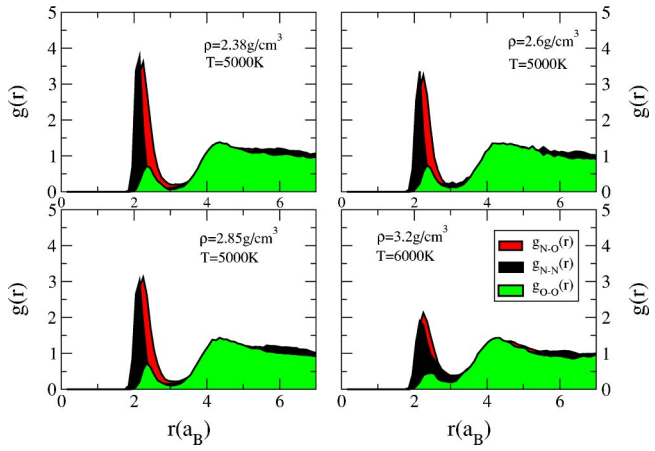

FIG. 4. (Color online) Pair-correlation functions along a second NO Hugoniot.

simulation results, we also point out that the QMD findings regarding the states of oxygen and nitrogen are also consistent with the behavior of pure molecular nitrogen and oxygen along their respective Hugoniots, where it is generally accepted that both species dissociate as the pressure and/or temperature increase.[22,26]

We now turn our attention to the nature of the fluid along the second-shock Hugoniot. Figure 4 shows the pair-correlation functions of the various diatomic species along the second-shock Hugoniot. As was mentioned above, we find that the temperature is almost constant at around 5200 K for the first three densities studied along the second-shock Hugoniot. Following the evolution of NO along the second-shock Hugoniot allows us to probe, as for pure nitrogen, the effect of increased density on the constituency of the fluid without the significant increase in temperature usually associated with shock measurements. This aspect could be particularly useful in the determination of Tersoff type potentials, such as the reactive empirical bond order potential,[14,15] where the bulk of the effort centers on accounting for the influence of density effects on the nature of the molecular bounds.

Figure 4 shows similar molecule concentrations for the reshock as for the principal Hugoniot. The pair-correlations functions calculated indicate, as before, a significant fraction of NO and N_2 as well as a very small fraction of molecular oxygen. Additionally, the initial density of the second-shock Hugoniot shown in Fig. 4 corresponds to the conditions of the first-shock Hugoniot where we have found that the concentration of molecular nitrogen is significant. Consequently, the initial state of the second-shock Hugoniot consists of a mixture of NO, N_2, and atomic oxygen while the second-shock Hugoniot describes the evolution of this particular media as the density increases. Figure 4 indicates that when the density increases along the second-shock Hugoniot, NO and N_2 dissociate but to a lesser degree than along the principal Hugoniot. This can be understood by the lower temperature of the second shock. Furthermore, we also see that the nitrogen pair-correlation function indicates that while dissociating as the density increases, a significant fraction of molecular nitrogen remains along the second shock and up to a density of 3.2 g/cm^3. This analysis of the nature of the fluid along the second-shock Hugoniot also sheds some light on the behavior of the second-shock temperature. We can indeed conclude that in addition to the large dissociation energy of the nitrogen oxide molecule, the formation of molecular nitrogen in the sample and its dissociation as the density increases also contributes to the small temperature variation found theoretically along the second-shock Hugoniot.

IV. CONCLUSION

We studied the high-pressure behavior of nitrogen oxide along the first and second-shock Hugoniots. We find that QMD provides a good description of the experimental data for both Hugoniots. As for other diatomic systems such as hydrogen, nitrogen, and oxygen, the increase in temperature along the principal Hugoniot presents a plateau corresponding to the dissociation of molecules in the media. This plateau is more pronounced for the second-shock Hugoniot where we find that the temperature remains mostly constant for initial conditions corresponding to the highest shock density reached experimentally. Finally, we find that for the overdriven conditions studied here, oxygen stays in an atomic state for the whole density range explored. We further find that while nitrogen is present in a molecular state for the lowest density studied, it eventually also dissociates as the density and temperature increase along both Hugoniots.

ACKNOWLEDGMENTS

We would like to thank J. D. Johnson, M. S. Shaw, L. Soulard, J. B. Maillet, and T. Gerrman for helpful discussions. This work was performed under the auspices of an agreement between CEA/DAM and NNSA/DP on cooperation on fundamental science. Work at LANL was performed under the auspices of the U.S. Department of Energy at Los Alamos National Laboratory under Contract No. W-7405-ENG-36.

[1] M. D. Knudson, D. L. Hanson, J. E. Bailey, C. A. Hall, J. R. Asay, and W. W. Anderson, Phys. Rev. Lett. **87**, 225501 (2001).
[2] G. W. Collins, L. B. DaSilva, P. Celliers, D. M. Gold, M. E. Foord, R. J. Wallace, A. Ng, S. V. Weber, K. S. Budil, and R. Cauble, Science **281**, 1178 (1998), and references therein.
[3] T. Lenosky, S. Bickham, J. Kress, and L. Collins, Phys. Rev. B **61**, 1 (2000).
[4] G. Galli, R. Hood, A. Hazi, and F. Gygi, Phys. Rev. B **61**, 909 (2000).
[5] S. Bagnier, P. Blottiau, and J. Clerouin, Phys. Rev. E **63**, 025301 (2001).
[6] Michael P. Desjarlais, Phys. Rev. B **68**, 064204 (2003).

[7] B. Militzer and D. Ceperley, Phys. Rev. Lett. **85**, 1890 (2000); B. Militzer and E. Pollock, Phys. Rev. E **61**, 3470 (2000).
[8] P. M. Celliers, G. W. Collins, L. B. DaSilva, D. M. Gold, R. Cauble. R. J. Wallace, M. E. Foord, and B. A. Hammel, Phys. Rev. Lett. **84**, 5564 (2000).
[9] M. Bastea, A. C. Mitchell, and W. J. Nellis, Phys. Rev. Lett. **86**, 3108 (2001).
[10] L. A. Collins, S. R. Bickham, J. D. Kress, S. Mazevet, T. J. Lenosky, N. J. Troullier, and W. Windl, Phys. Rev. B **63**, 184110 (2001).
[11] S. Mazevet, J. D. Kress, L. A. Collins, and P. Blottiau, Phys. Rev. B **67**, 054201 (2003).
[12] S. Mazevet, L. A. Collins, N. H. Magee, J. D. Kress, and J. J. Keady, Astron. Astrophys. **405**, L5 (2003).
[13] G. L. Schott, M. S. Shaw, and J. D. Johnson, J. Chem. Phys. **82**, 4264 (1985).
[14] M. L. Elert, D. M. Deaven, D. W. Brenner, and C. T. White, Phys. Rev. B **39**, 1453 (1989).
[15] D. W. Brenner, O. A. Shenderova, J. A. Harrison, S. J. Stuart, B. Ni, and S. B. Sinnott, J. Phys.: Condens. Matter **14**, 783 (2002).
[16] M. S. Shaw, *Shock Compression of Condensed Matter*, edited by S. C. Schmidt, R. D. Dick, J. W. Forbes, and D. G. Tasker (Elsevier, New York, 1992), Vol. 131.
[17] G. Kresse and J. Hafner, Phys. Rev. B **47**, RC558 (1993); G. Kresse and J. Furthmüller, Comput. Mater. Sci. **6**, 15 (1996); G. Kresse and J. Furthmüller, Phys. Rev. B **54**, 11169 (1996).
[18] D. Vanderbilt, Phys. Rev. B **41**, 7892 (1990).
[19] G. Kresse and J. Hafner, J. Phys.: Condens. Matter **6**, 8245 (1994).
[20] J. P. Perdew, in *Electronic Structure of Solids*, edited by F. Ziesche and H. Eschrig (Akademie Verlag, Berlin, 1991).
[21] J. D. Kress, S. Mazevet, L. A. Collins, and W. W. Wood, Phys. Rev. B **63**, 024203 (2001).
[22] S. Mazevet, J. D. Johnson, J. D. Kress, L. A. Collins, and P. Blottiau, Phys. Rev. B **65**, 014204 (2002).
[23] Ya. Zeldovich and Yu. Raizer, *Physics of Shock Waves and High-Temperature Hydrodynamic Phenomena* (Academic Press, New York, 1966).
[24] W. J. Nellis and A. C. Mitchell, J. Chem. Phys. **73**, 6137 (1980); W. J Nellis, N. C. Holmes, A. C. Mitchell, and M. van Thiel, Phys. Rev. Lett. **53**, 1661 (1984).
[25] W. J. Nellis, H. B. Radousky, D. C. Hamilton, A. C. Mitchell, N. C. Holmes, K. B. Christianson, and M. van Thiel, J. Chem. Phys. **94**, 2244 (1991).
[26] J. D. Kress, S. Mazevet, and L. A. Collins, in *Shock Compression of Condensed Matter–2001*, edited by Michael D. Furnish, Yuki Horie, and Naresh N. Thadhani, AIP Conf. Proc. No. 620 (AIP, Melville, NY, 2002), p. 91.
[27] M. J. Frisch *et al.*, GAUSSIAN 98, Rev. A.2 (Gaussian, Inc., Pittsburgh, PA, 1998).
[28] K. P. Huber and G. Herzberg, *Molecular Spectra and Molecular Structure. IV. Constants of Diatomic Molecules* (Van Nostrand-Reinhold, New York, 1979).